An Experimental Study of Volumetric Quality on Fluid Flow and Heat Transfer Characteristics for Two Phase Impinging Jets

by

Brian K. Friedrich II

Submitted in Partial Fulfillment of the Requirements

for the Degree of

Master of Science

in the

Mechanical Engineering

Program

YOUNGSTOWN STATE UNIVERSITY

May, 2016

The Influence of Volumetric Quality on the Circular Hydraulic Jump of Air-Assisted Jet Impingement

Brian K. Friedrich II

I hereby release this thesis to the public. I understand that thesis will be made available from the OhioLINK ETD Center and the Maag Library Circulation Desk for public access. I also authorize the University or other individuals to make copies of this thesis as needed for scholarly research.

Signature:

_____

Brian K. Friedrich II, Student Date

Approvals:

_____

Kyosung Choo, Thesis Advisor Date

_____

Guha Manogharan, Committee Member Date

_____

Jae Joong Ryu, Committee Member Date

_____

Dr. Salvatore A. Sanders, Dean of Graduate Studies Date

ABSTRACT

This study further expands the current knowledge of the relationship between heat transfer and fluid mechanics. Fluid flow and heat transfer characteristics of air-assisted water jet impingement was experimentally investigated under a fixed water flow rate condition. Water and air were the test fluids. The effects of volumetric quality ($\beta = 0 - 0.9$) on the Nusselt number, hydraulic jump diameter, and pressure were considered. The results showed that stagnation Nusselt number, hydraulic jump diameter, and stagnation pressure increased with volumetric quality to a maximum value at 0.8 of the volumetric quality, and then decreased. The stagnation Nusselt number and hydraulic jump diameter of the air-assisted water jet impingement are governed by the stagnation pressure. Based on the experimental results, a new correlation for the normalized stagnation Nusselt number and hydraulic jump are developed as a function of the normalized stagnation pressure alone. This research can be applied to further enhance the cooling of industrial applications, such as, cooling of electronics and processing of materials.

CONTENTS

NOMENCLATURE

d	nozzle diameter [m]
L	nozzle length [m]
d_{hj}	hydraulic jump diameter [m]
d_{hj}/d	dimensionless hydraulic jump diameter [-]
P_{stag}	pressure measured at stagnation point [kPa]
P^*_{stag}	normalized pressure [-]
ΔP	pressure drop [Pa]
Q	flow rate [m^3/s]
Re	Reynolds number [ud/v]
r_{hj}	radius measured from jet stagnation point [m]
u	jet velocity [m/s]
H	nozzle to plate height [m]

Subscripts

hj	hydraulic jump
stag	stagnation point
w	water

Superscripts

*	Dimensionless number

LIST OF FIGURES

PAGE

CHAPTER I

INTRODUCTION AND BACKGROUND

A hydraulic jump is a hydraulic phenomenon which is frequently observed in rivers and canals. It can also be seen in everyday situations as shown in an example of this in an ordinary household hose in Figure 1.

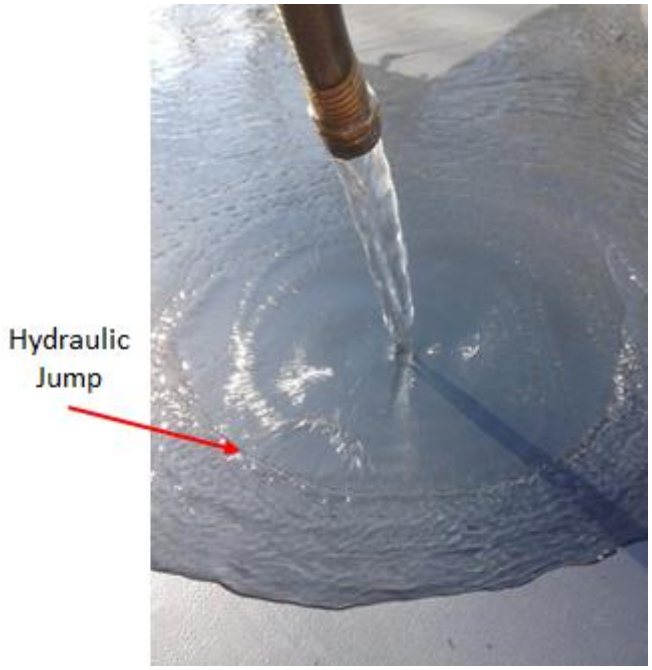

Figure 1: Hydraulic jump caused by an ordinary household hose.

When liquid at higher velocity discharges into a zone of lower velocity, a rather abrupt rise occurs in the liquid surface. This phenomenon is dependent mainly on the initial fluid speed. If the initial speed of the fluid is below the critical speed, then hydraulic jump will not occur. When initial flow speeds are higher than the critical speed, hydraulic jump occurs. When a water jet impinges on a horizontal plate, a circular hydraulic jump is formed

at a certain distance away from the jet impact point. Boundary conditions upstream and downstream of the jump will dictate its strength, which determines the type of hydraulic jump and its stability. Figure 2 shows an example of a sluice gate which depicts a hydraulic jump and corresponding components, ME Case Studies, 2011.

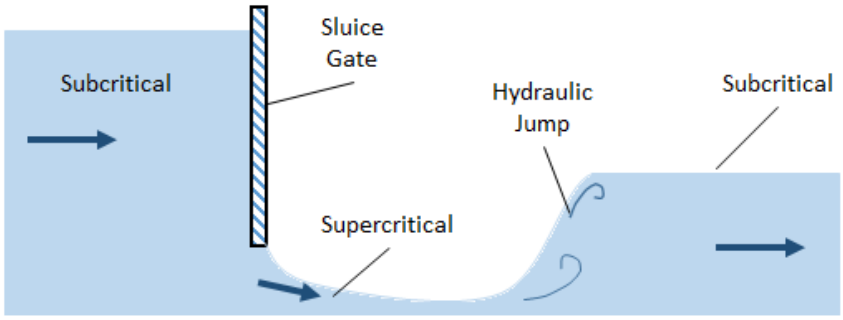

Figure 2: Hydraulic jump diagram.

The determination of the diameter of hydraulic jump is very important since the heat transfer characteristics of impinging jets are drastically changed at the location of hydraulic jump, as mentioned by previous researchers (Stevens and Webb, 1991; Baonga et al., 2006; Liu and Lienhard, 1993). Due to the importance of hydraulic jump, extensive studies on the heat transfer and hydrodynamics of hydraulic jumps for single-phase impinging jets have been reported in the literature (Chanson, 2009; Godwin, 1993; Louahlia-Gualous and Baonga, 2008; Watson, 1964; Craik et al., 1981; Zhao and Khayat, 2008; Mikielewicz and Mikielewicz, 2009; Chang et al., 2001).

In this research, the hydraulic jump is created by the use of an impinging jet. An impinging jet is a liquid or gaseous flow which is directed by a nozzle and discharged at a surface. The impinging jet used in this research is an unsubmerged jet where the fluid passes through a gas before it impinges on the surface. When the jet hits the surface it creates a laminar region as shown in Figure 2 which transforms into a hydraulic jump.

Impinging jets are extremely efficient at transferring large amounts of thermal energy or mass between the surface and the field. In high heat transfer applications where a large heat load needs to be removed, an impinging jet is an attractive solution due to its high heat flux. These high heat fluxes mostly depend on the velocity of the jet which will produce a high stagnation pressure, Chang et al, 2001. The high pressure creates a laminar region after the impinging zone which offers a high heat transfer coefficient. This heat transfer coefficient can be three times larger than other conventional convection cooling, such as parallel flow, Lienhard, 2001. Some examples of applications of an impinging jet are in drying foods, cooling processed materials, cooling of electronics, cooling of turbine engines, cooling during machining and similar industrial processes. A schematic diagram illustrating the different regions of an impinging jet are shown in Figure 3, Incropera and DeWitt, 2002.

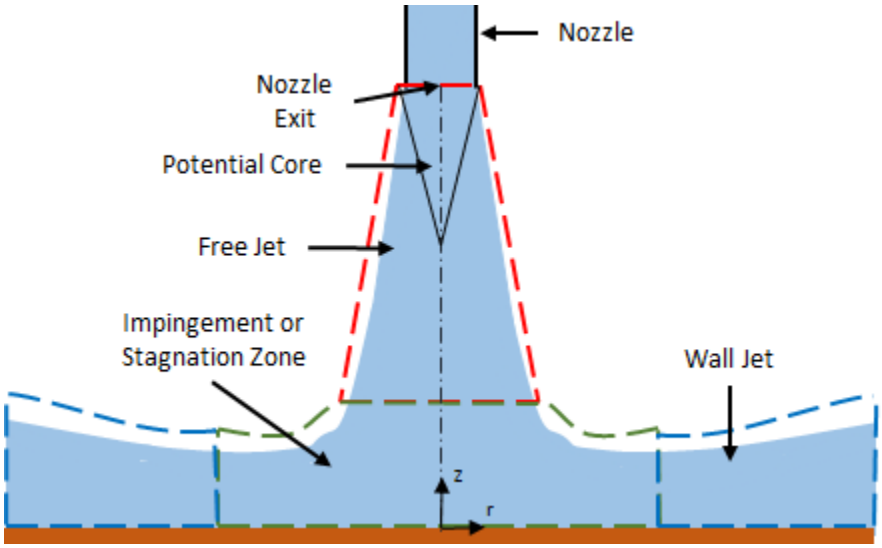

Figure 3: Impinging jet diagram.

This experiment focuses on the fluid flow and heat transfer of two phase liquids. It is important that a proper understanding of the mechanics of fluids and heat transfer is

required to understand the correlations of heat transfer and fluid flow. Heat transfer is the rate of which energy that can be transferred from one system to another. The energy transfer is caused by the temperature difference between systems, Cengel and Ghajar, 2011. This research focuses on convection. Convection is the governing parameter for the heat transfer testing. In forced convection, the fluid is forced over a surface by an external means, as an example is shown in Figure 4. This means that forced convection is closely tied with fluid mechanics, Cengel and Chajar, 2011.

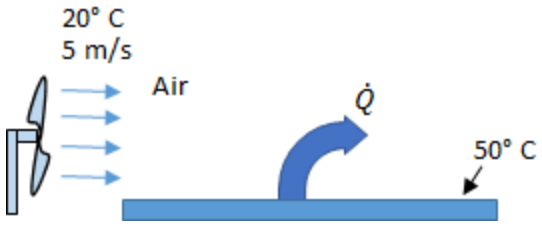

Figure 4: Forced convection example.

Fluid motion enhances convection heat transfer, when it forces a warmer or cooler fluid into contact with a surface, initiating higher rates of conduction at more areas in a fluid. Hence, greater the fluid velocity, higher the rate of heat transfer. Heat transfer through convection the flowing equation can be expressed as:

$$\dot{Q} = hA_s(T_s - T_\infty) \tag{1}$$

where h is the convection heat transfer coefficient (W/m^{2}K), A_s is the heat transfer surface area (m^2), T_s is the surface temperature (ºC), and T_∞ is the fluid temperature (ºC). The convection heat transfer coefficient is defined as the rate of heat transfer between a solid surface and a fluid per unit surface area per unit temperature difference. In the case of convection, it is important to look at the ratio of convective to conductive heat transfer across the boundary (surface). This ratio creates a dimensionless coefficient called the Nusselt number, *Nu*. Nusselt number is defined in the following equation:

$$Nu = \frac{hL_c}{k} \quad (2)$$

Where k is the thermal conductivity of the fluid (W/mK) and L_c is the characteristic length (m). The Nusselt number represents the degree of increase in heat transfer through a fluid layer as a result of convection relative to conduction across the same fluid layer, (i.e.) higher *Nu* leads to more effective convection, Cengel and Ghajar, 2011.

It is important review prior research to gain a better understanding of the relationship between hydraulic jump diameter and Nusselt number relate. Stevens and Webb, 1991 studied the flow structure of a water film formed by a single-phase circular jet impinging perpendicularly on a horizontal surface. This experimental study was performed using nozzle diameters in the range of 2.2–8.9 mm and Reynolds number in the range of 1,000–52,000. The dimensionless hydraulic jump diameter was suggested to be a function of Reynolds number: $r_{hj}/d = 0.0061\mathrm{Re}^{0.82}$. Baonga et al., 2006, conducted an experimental study on the hydrodynamic and thermal characteristics of a free liquid single-phase jet impinging on a heated disk. They performed experiments using nozzle diameters of 2.2 and 4 mm and Reynolds numbers in the range of 600–9,000. An empirical correlation for the dimensionless hydraulic jump diameter was suggested as a function of Reynolds number: $r_{hj}/d = 0.046\mathrm{Re}^{0.62}$. Liu and Lienhard, 1993, performed an experimental study for a nozzle diameter of 4.96 mm. The effects of Reynolds number, Weber number (ratio of inertial forces compared to surface tension), and Froude number (ratio of flow inertia compared to gravity forces) on the dimensionless hydraulic jump diameter of single-phase impinging jet were investigated. Choo and Kim, 2016, conducted an experimental study on the effects of nozzle diameter on hydraulic jump diameter. They showed that dimensionless hydraulic jump diameter is independent of the nozzle diameter under fixed

pumping power conditions and that the dimensionless hydraulic jump diameter increases with decreasing nozzle diameter under fixed jet Reynolds number conditions. Even though there are several past studies in this topic, the effect of volumetric quality on the hydraulic jump diameter has not been thoroughly studied for two phase impinging jets. Chang et al, 2001, looked at the hydraulic jumps based on boundary layer separation. They investigated the hydraulic jump diameter as a function of a modified Froude number, the jet Reynolds number, and jet diameter.

Surface topology and the fluid were used as key factors in the distortion and preservation of a hydraulic jump as researched by Johnson, 2014; Maynes, 2011; and Bush, 2006. Johnson, 2014, and Maynes, 2011, showed that a normal circular hydraulic jump can be altered by changing the roughness and surface topology of the impinging surface. The researchers studied hydrophilic, hydrophobic, and super-hydrophobic surfaces which exhibit alternating microribs and cavities for a single-phase liquid impingement. It was found that the hydraulic jump would elongate in the direction of least resistance there by deforming the normal circular hydraulic jump into an elliptical cross section. Bush, 2006, analyzed the effects of different fluids impingement on smooth surfaces. It was found that fluids with higher viscosity than water can deform the hydraulic jump into a polygonal structure due to capillary instability.

A range of studies on applications of impinging jets have been performed. Webb and Ma, 1995; Viskanta, 1993; Martin, 1977; and Polat et al., 1989 all researched single phase impinging jet flow for heat transfer characteristics. Lytle and Webb, 1994, studied impinging jet flow at low nozzle-plate spacing, (i.e.) h/d of 6 to 0.1. They found that decreasing nozzle height increases the heat transfer rate. Lee et al., 2015, researched the effect of single phase impinging flow on concave and convex impinging surfaces for heat

transfer characteristics. They found that the Nusselt numbers for the concave surface are higher than those for the convex surface at all of the Reynolds numbers tested. Gardon and Akfirat, 1966 and 1965, studied submerged air jets and the heat transfer rates at the impinging zone. They also expanded their research to study turbulent flow which can take place in the submerged jet. It was shown that some seemingly irregular heat-transfer phenomena can be explained as effects of the intense and spatially varying turbulence inherent in jets. This research was applied to electronic cooling in the paper by Garimella, 1996. A confined impinging jet is another class of jet where the impinged fluid is pushed into a channel the same height as the nozzle. Obot et al., 1982; Baydar and Ozmen, 2006, and Pence et al., 2003, experimentally and numerically studied semi and fully confined impinging jets. They found that confining a jet can reduce the heat transfer coefficients of the impinging jets as compared to a free jet. Akansu et al., 2003, Abdel-Fattah and El-Baky, 2009; Beitelmal et al., 2000; and Yan and Saniei, 1997, studied both numerical and experimental for inclined impinging surfaces. They determined that when the angle is increased the largest heat transfer rate was found further uphill of the impinging zone. Another study was done to analyze the fluid flow of a twin impinging jet which could vary in height and attack angle. This study conducted by Abdel-Fattah, 2007, concluded that the recirculation zone between the jets it directly related to the attack angle and height of the nozzle from the impinging jets. Research done by Al-Hadhrami, 2010; Al-Hadhrami et al., 2007; and Mubarak et al, 2011 further experimentally studied the twin impinging jet and the heat transfer characteristics of staggering and single row jet arrays. Micro-scale impinging jets are becoming more popular for electrical component cooling. Goldstein and Franchett, 1988 created a numerical model to show that on the micro scale the testing fluid is still considered to be incompressible.

Several researchers have observed heat transfer enhancement resulting from the addition of a gas (or vapor) phase in an impinging liquid jet which is considered a two-phase flow. Trainer et al., 2013, investigated the effect of nozzle diameter on heat transfer characteristic of the impinging jet and showed that heat transfer of the air-assisted jets was enhanced by almost 260%. Hall et al., 2001, performed an experimental study on boiling heat transfer for air-water impinging jets. Heat transfer was increased by as much as 210% at the stagnation point for the volumetric fraction ranging from 0 to 0.4 and the liquid-only Reynolds number of $11{,}300 \leq Re_w \leq 22{,}600$. Zumbrunnen and Balasubramanian, 1995, observed the enhancement in convection heat transfer caused by air bubbles injected into a planar water jet. Heat transfer was increased by almost 220% at the stagnation point over the range of liquid-only Reynolds number of $3{,}700 \leq Re_w \leq 21{,}000$ and the volumetric fraction between $0 \leq \beta \leq 0.86$. Serizawa et al., 1990, experimentally studied the heat transfer characteristics of an impinging circular jet of an air-water mixture for Reynolds numbers in the range $25{,}000 < Re_w < 125{,}000$. Heat transfer coefficient was increased by almost 200% at a volumetric fraction of 0.53. Chang et al., 1995, experimentally investigated the heat transfer characteristics of confined impinging jets using Freon R-113. When compared to a single-phase jet, heat transfer of the liquid-vapor jets was enhanced by a factor of 1.2. Choo and Kim, 2010, studied the heat transfer effects of an air-assisted impinging jet and obtained an optimum point, $\beta=0.2$, under a fixed pumping power condition. These researchers also noted that this enhancement had some implications. It was only feasible at operating conditions of a high pump power, due to systems' pressure drop and required flow rate. In addition, as the volumetric quality of the testing fluid at a constant flow rate was increased, the required power for pumping also increased as a direct result of increased pressure drop.

Even though there have been prior studies on two phase impinging jets, the effect of volumetric quality on the relationship of Nusselt number, hydraulic jump, and stagnation pressure for two-phase impinging jets have not been thoroughly studied (or understood).

The goal of this research is to determine the effects of volumetric quality of water with a constant flow rate on hydraulic jump diameter, stagnation pressure and Nusselt number for two phase impinging jets. The hydraulic jump diameter and stagnation pressure were analyzed to understand their relationship to heat transfer characteristics. The working fluids are air and water (single phase, i.e. water is used as a reference and validation for the experiment). Four different Re of water (3,030, 3,463, 3,896, and 4,329) are tested as each of the volumetric qualities increase from $\beta = 0 - 0.9$. Based on these experimental results, a new correlation for the dimensionless hydraulic jump diameter (d_{hj}/d) was developed as a function of normalized stagnation pressure (P^*_{stag}) alone. Further, the experimental results show a new correlation for the normalized stagnation Nusselt number is developed as a function of the normalized stagnation pressure alone. In addition, it is found that the lateral variation of Nusselt number is governed by hydraulic jump size. Findings from this study can be applied to cooling applications (i.e.) electronics cooling. The organization of this thesis includes: Chapter 2 describes the experimental approach; Chapter 3 describes the results and discussion; Chapter 4 describes the conclusion and future directions.

CHAPTER II

EXPERIMENTAL APPROACH

The hydraulic jump diameter, pressure, stagnation and lateral Nusselt number caused by single and two phase flow from an impinging jet were measured for a dimensionless jet-to-surface of H/d = 1 and Reynolds numbers in the nominal range of 3030 – 4329.

2.1 FLOW SYSTEM

A schematic of the flow path for both air and water is shown in Figure 7. Compressed air and water was supplied with flexible tubing before entering the two-phase mixer. The airflow was supplied from a high-pressure tank to ensure a clean and steady flow rate using a pressure regulator. The flow was regulated and controlled using a mass flow controller (Omega FMA5520A), Figure 12, having an accuracy of ±1% and a repeatability of ±0.15%. The full-scale range of the mass flow controller that was used was 10 standard liters per minute. Water was the working liquid. A commercial water line was used to supply the water. The liquid flow was regulated and controlled using flowmeter valves (Dwyer RMC-135-SSV and Dwyer RMB-82D-SSV), as shown in Figure 15.

2.2 TEST ENVELOPE

A circular, extruded acrylic nozzle which produced the impinging jet was used in the experiment after the two phase mixer. It was 470 mm long with a diameter of 5.86 mm. The circular nozzle was fixed on a 3-axis (x-y-z) stage with a 10 µm resolution, (Thorlabs, Inc, PT3A/M). The nozzle exit was positioned 5.86 mm above the impinging surface to give an $H/d = 1$. A digital manometer (Dwyer Series 490-2) was used to measure the wide range of pressures from the impinging jet's stagnation zone. The manometer has a range of 0 – 30 kPa with an accuracy of ±0.5%, shown in Figure 13. The stagnation pressure of the impinging jet was measured between the stagnation zone and the atmospheric pressure. The flow system was not changed when changing from the fluid flow experiment to the heat transfer experiment for uniformity to the tests.

A schematic of the test section is presented in Figure 8. The test envelope was constructed using transparent acrylic sheets. The impingement surface was designed to be at a greater elevation than the pool bottom such that the impinged liquid would fall off the impinging plate and into the pool. This eliminates disturbances from the impinging fluid on downstream flow. The circular impinging plate was fabricated using transparent acrylic sheet with a thickness of 5.15 mm, 216 mm diameter and 1 mm diameter orifice. The orifice was connected to the manometer using flexible tubing. The hydraulic jump created on the impinging plate was measured using standard digital Vernier calipers and verified using photo measurement techniques.

A schematic of the test section for the heat transfer experiment is presented in Figures 9-11. The heater was made of stainless steel (0.0508 mm thick, 12.5 mm wide and 192.8 mm long). The heater was connected to a high voltage DC power supply (Agilent 6651A #J03) in series with a shunt, rated 0-6 V and 0-60 A, and copper bus bars allowing

adjustable DC voltage to the electrodes. With DC electric current applied to the heater, a nearly uniform wall heat flux boundary condition was established. The amount of heat generation was recorded under steady state condition.

A 12.7 mm thick PTFE Teflon disk was used to mount the heater, thermocouples, and copper bus. The Teflon disc also provides insulation to minimize heat loss through the dry side of the heater. Five K-type thermocouples (with a max service temperature of 260°C) of diameter 0.08 mm were fixed through 1 mm mounting holes on the centerline of the Teflon disk by a high temperature thermal epoxy. The thermocouples were spaced 21.5 mm apart starting at the center point. A thin double sided adhesive strip was laid directly over the row of thermocouples. The heater was then laid on top of the adhesive strip to keep constant contact with the thermocouples, Choo and Kim, 2010; Friedrich et al., in prep; Choo and Kim, 2011; Choo et al., 2016. These thermocouples were connected to an OMEGA OM-CP-QuadTemp2000 digital data acquisition system (DAQ). The DAQ was connected to a computer where the real time temperatures were recorded. A heat resistant latex caulking (Nelson Latex Firestop Sealant) was used to seal any gaps created due to the machining of the Teflon disk. The flow patterns in the pipe nozzle and on impinging surface were captured by using a digital camera (Nikon, D50) and a pulse generator (Fovitec - Speedlight flash, KD560) which were synchronized to work together, Baydar and Ozmen, 2006; Pence and Boeschoten, 2003. The data analysis followed the guidelines given in, Choo and Kim, 2010; Friedrich et al., in prep; Choo and Kim, 2011; Choo et al., 2016. The temperature data given from the DAQ, power provided from the DC power supply, resistance and surface area across the heater surface, and the fluid properties were used to calculate (using equations 1 and 2) the Nusselt number at each Reynolds number.

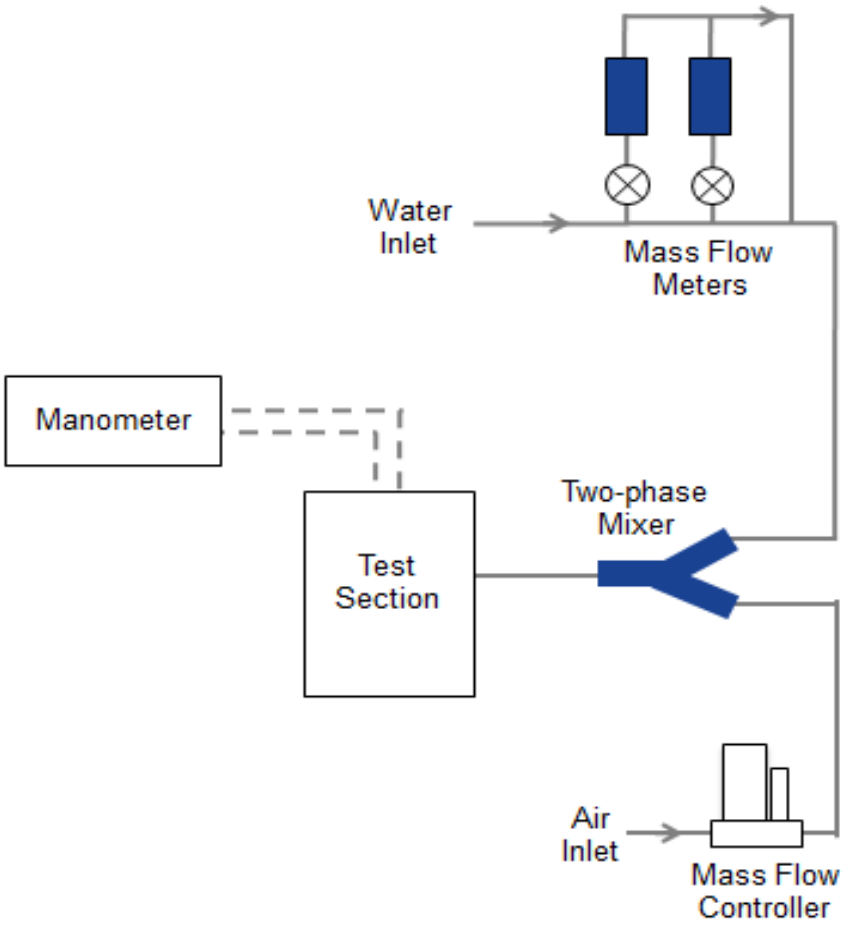

Figure 5: Schematic diagram of experimental set-up.

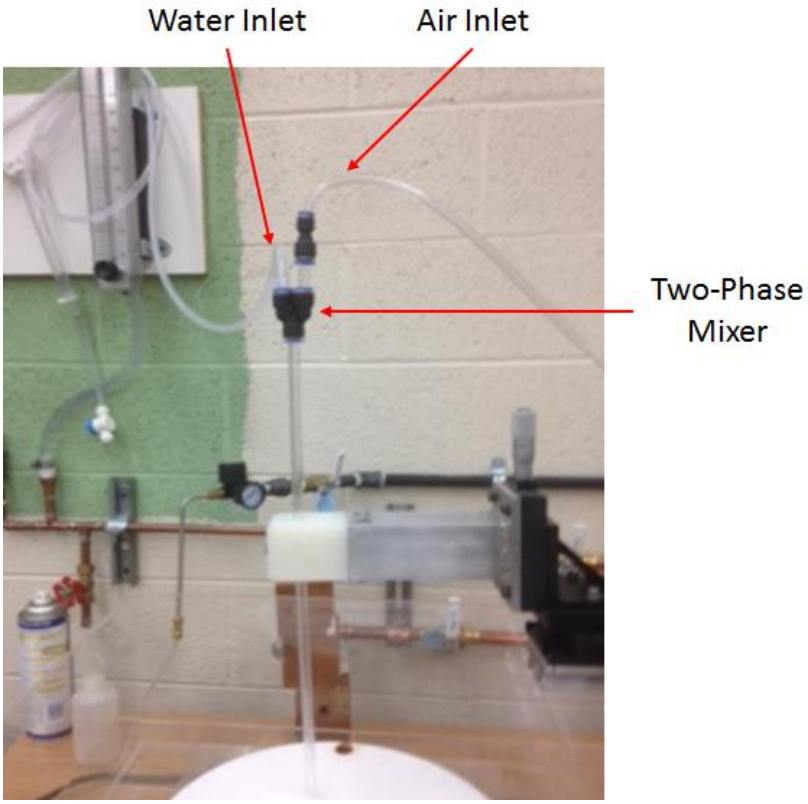

Figure 6: Two-phase mixer used in experiment.

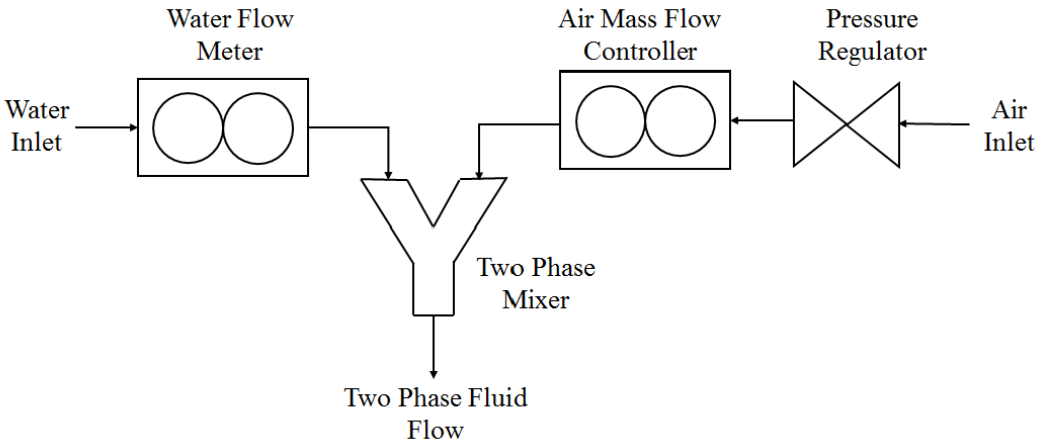

Figure 7: Schematic of test loop for air and water.

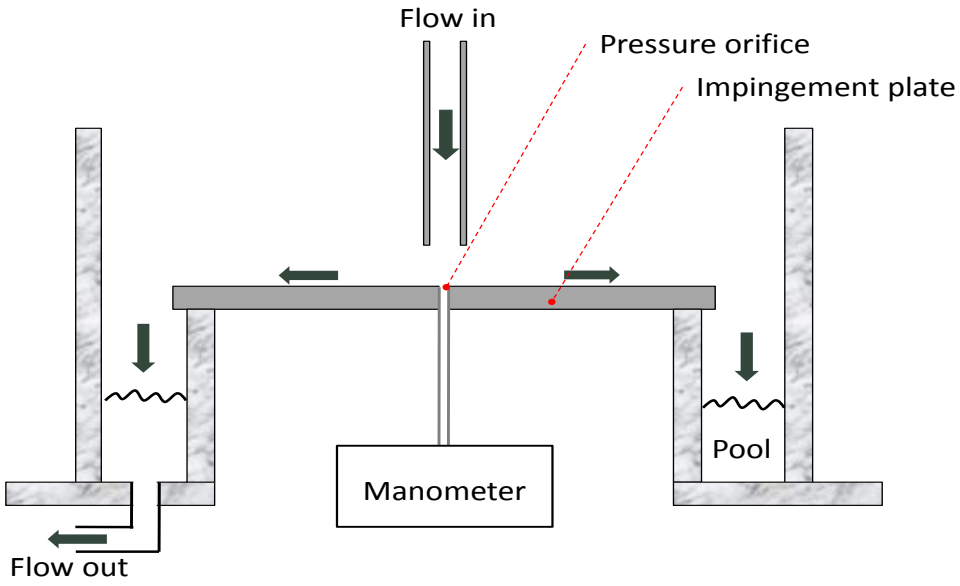

(a)

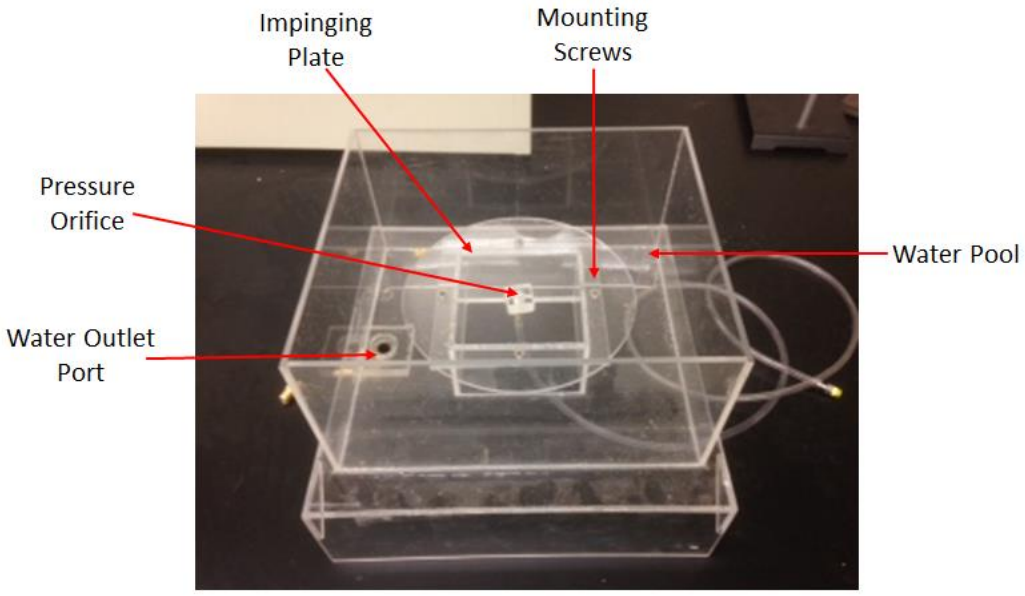

(b)

Figure 8: Fluids test section configuration: (a) cross sectional diagram of the test section and (b) actual test section used in the experiment.

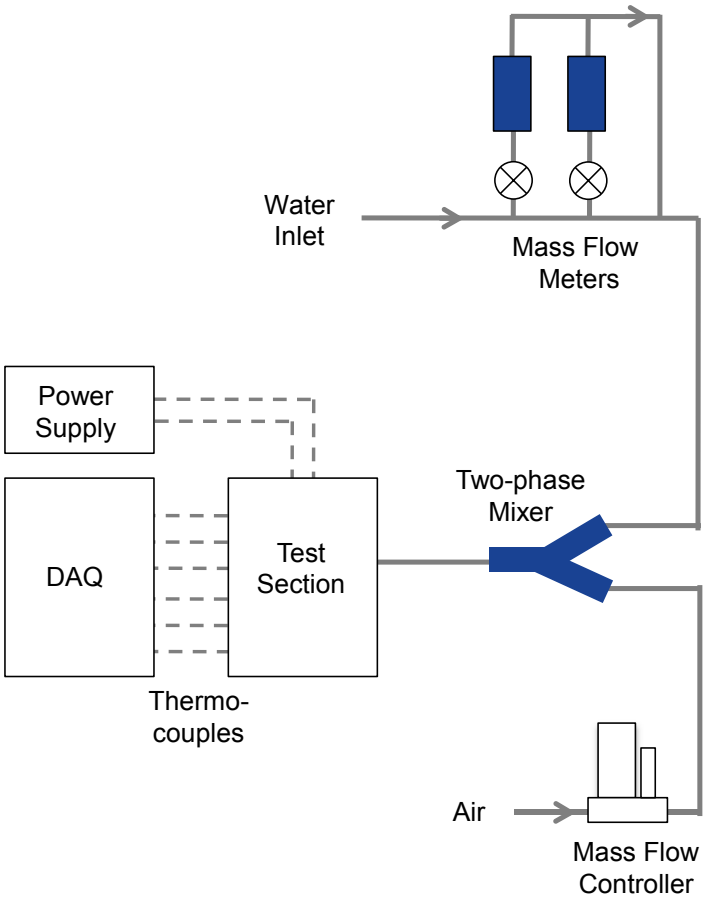

Figure 9. Schematic diagram of heat transfer experimental set-up.

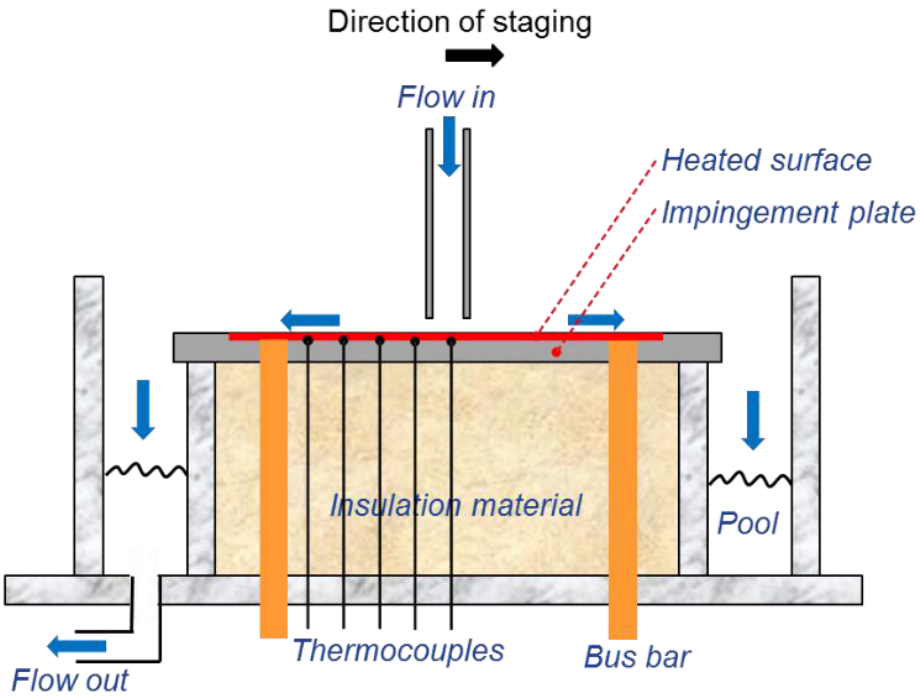

(a)

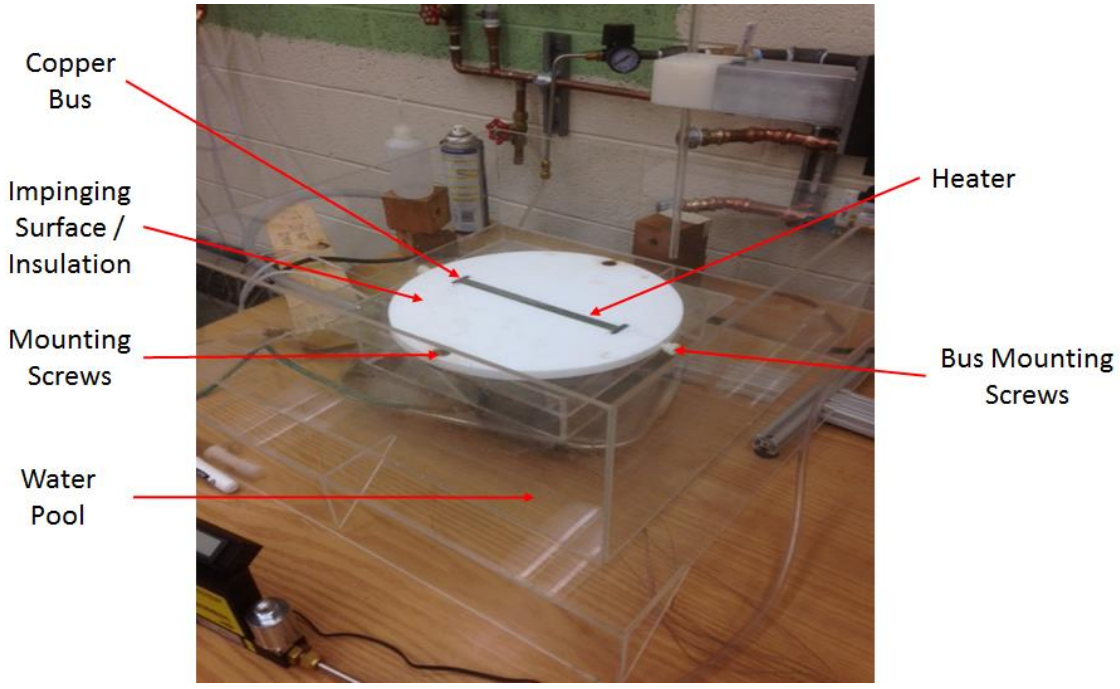

(b)

Figure 10: Heat transfer test set-up configuration: (a) cross sectional diagram of the test section and (b) actual test section used in the experiment.

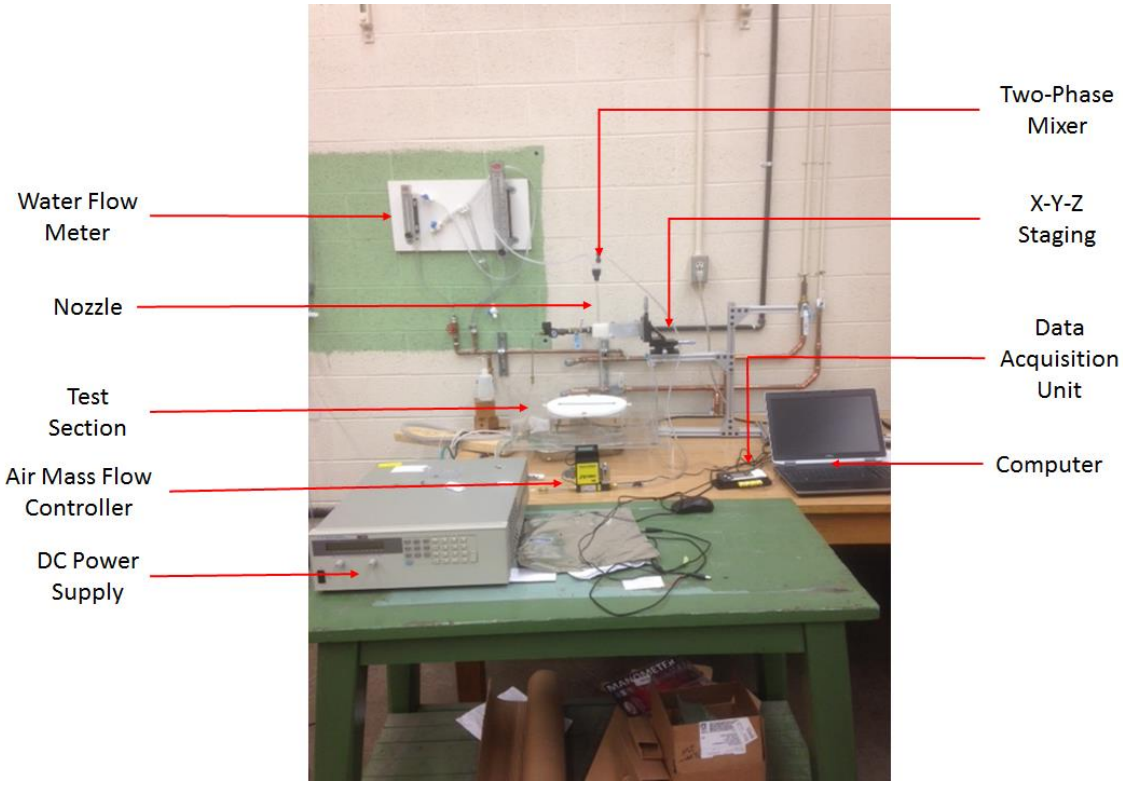

Figure 11: Heat transfer overview of experimental test set-up.

Figure 12: Mass flow controller.

Figure 13: Manometers.

Figure 14: Air inlet with pressure regulator.

Figure 15: Water flow controller.

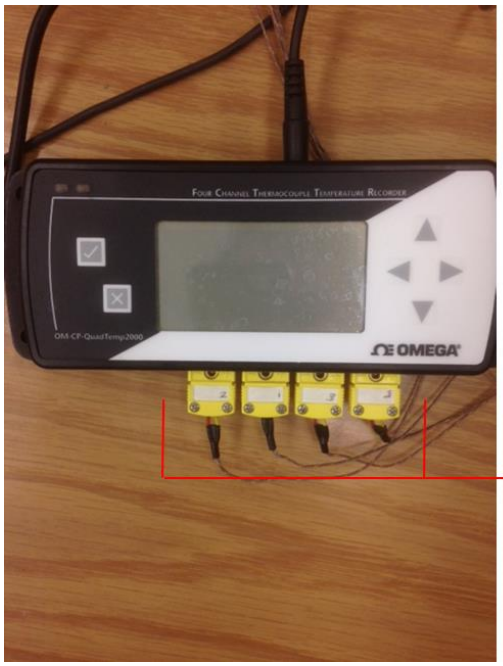

Figure 16: Data acquisition unit.

2.3 PROCEDURE

In order to establish steady-state of the fluid flow characteristics experiments, 5 minutes intervals between each flow rate change for different volumetric qualities were provided. Both hydraulic jump and stagnation pressure were measured with minimum, actual, and maximum values at the steady state time. Standard digital Vernier calipers were used to measure the hydraulic jump diameter. It was crucial to measure the hydraulic jump at the same level for each test in order to minimize error measurements. The tests were repeated 4 times for each Reynolds number of water. The manometer was recalibrated after every change in Reynolds number of water to ensure the quality of the results gathered from the testing.

The heat transfer tests started by impinging the fluid onto the heater surface, then applying the voltage to the heater. The voltage was set at 6V for this experiment. Before any results could be gathered the variation of the temperature difference between the heater and the nozzle exit needed to be within ±0.2 ºC for 10 min, before recording the temperature value. Subsequently, the voltage and resistance across the heater was measured in order to obtain electrical energy input accurately. To get more data points for each volumetric quality the staging was moved twice tangentially, 7.166 mm, from the stagnation thermocouple. Moving the staging allowed the 5 fixed thermocouples to now record 15 unique lateral locations with 7.166 mm spacing between each location. Such that the nozzle was 14.3 mm away from the stagnation thermocouple at the last position. The uncertainty in the local Nusselt numbers is estimated with a 95 percent confidence level using the methods suggested by Kline and McKlintock, 1953. Their methods calculate the uncertainty using the tolerances of the equipment being used in the experiment. The calculated maximum error of the main variables revealed an uncertainty of 2.7% for the

surface temperature with 1.9%, 1.2% for the inlet temperature at the nozzle exit, 1.1% for the heat loss, 1.1% for the input voltage, and 0.6% for the input current.

CHAPTER III

RESULTS AND DISCUSSION

3.1 VALIDATION

Validation for the dimensionless hydraulic jump radius comes from the comparison of the single phase liquid impingement data from previous experiments by Stevens and Webb, 1991, and Choo and Kim, 2016, as shown in Figure 17. A nozzle diameter of 5.86 mm and jet Reynolds numbers between 3,000 and 15,000 were examined. The present data agrees with the experimental results of the previous experiments within ±20%.

Validation for the Nusselt number comes from the comparison of the single phase liquid impingement data from previous experiments by Webb and Ma, 1995, as shown in Figure 18. A nozzle diameter of 5.86 mm and jet Reynolds numbers between 3,030 and 4,329 were examined. The present data agrees with the experimental results of the previous experiments within ±10%.

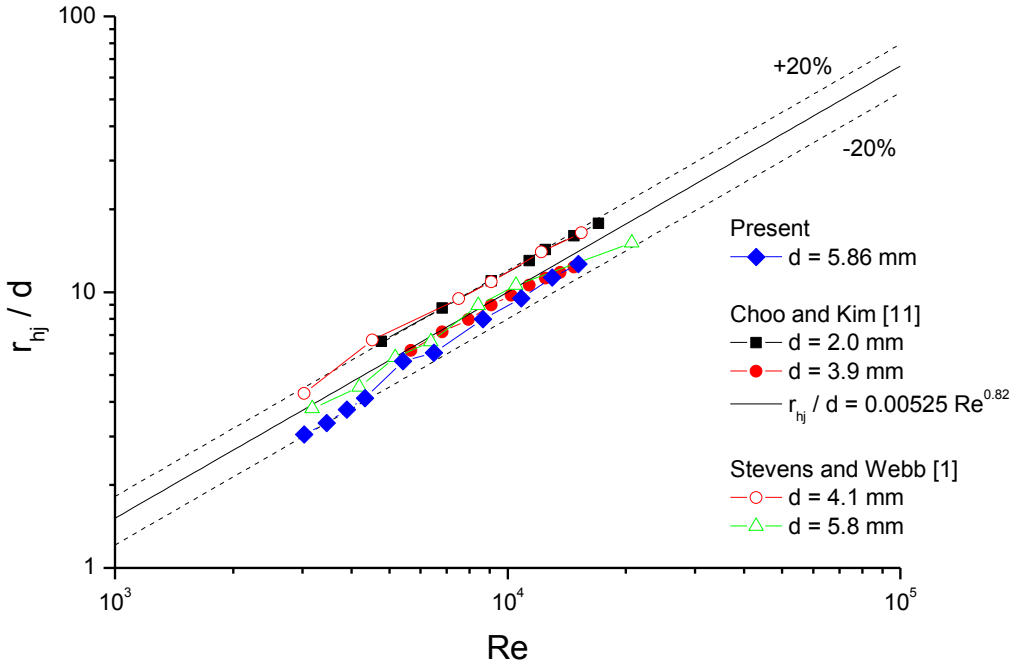

Figure 17: Comparison between present data and previous data for the hydraulic jump.

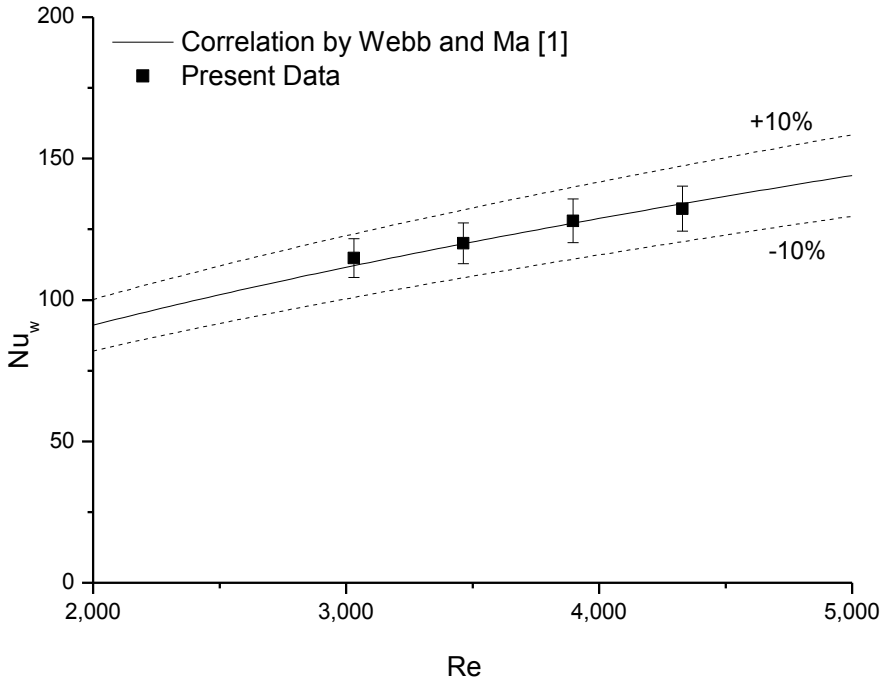

Figure 18: Comparison between present data and previous data for Nu.

3.2 HYDRAULIC JUMP DIAMETER AND PRESSURE

The variation of dimensionless hydraulic jump diameter and dimensionless stagnation pressure with changing volumetric quality are shown in Figures 19 and 20. The results are categorized into three regions; Region I is from $\beta = 0$ to $\beta = 0.4$, Region II is from $\beta = 0.4$ to 0.8, Region III is from $\beta = 0.8$ to $\beta = 0.9$.

Region I in the dimensionless hydraulic jump diameter and the stagnation pressure show a linear increase as β increases towards Region II. This section of d_{hj}/d and P_{stag} has a relatively gradual trend when compared to Regions II and III. The fluid flow pattern can be seen in Figure 21(a) and (b). The fluid flow of the hydraulic jump and the free jet zone at this range looks very similar to a pure water impingement. The stagnation zone can be easily compared between $\beta = 0$ and $\beta = 0.2$, which appears to be unaltered by the low β values. A majority of the bubbles also remain intact as they pass the laminar region at this lower β value.

In Region II, there was an exponential increase in the hydraulic diameter and the stagnation pressure until β reached 0.75 - 0.81. At this point a peak was reached indicating that at a certain volumetric quality a maximum pressure and hydraulic jump diameter can be found. The hydraulic jump diameter doubled in this range than that of single phase value. There were also a greater number of visible bubbles which stayed intact past the impingement zone and into the hydraulic jump. Figure 21(c) shows the flow pattern in Region II at $\beta = 0.6$. This figure shows an enlarged hydraulic jump diameter compared to both $\beta = 0$ and $\beta = 0.2$. This region also had a minor fluctuating hydraulic jump diameter.

Region III appears after a volumetric quality of $\beta = 0.8$. A sharp decrease in both pressure and hydraulic jump diameter can be seen in this region. This can be due to the water jet column distortion as it exits the nozzle, Figure 21(d), which increases the

stagnation zone size and causes the pressure to be lower, thus, creating a smaller dimensionless hydraulic jump. Bubbles were also intact after the impinging zone and hydraulic jump. This region had a larger fluctuating hydraulic jump diameter caused by water jet column distortion with high air velocity. These trends were found in each of the tested fixed flow rates.

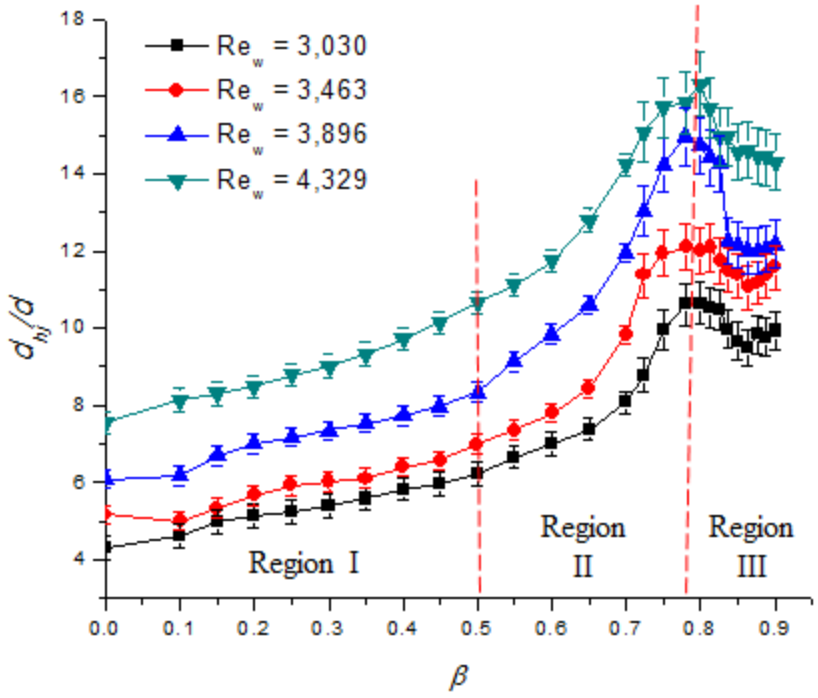

Figure 19: Dimensionless hydraulic jump diameter as a function of the volumetric quality.

Figure 20: Dimensionless stagnation pressure as a function of the volumetric quality.

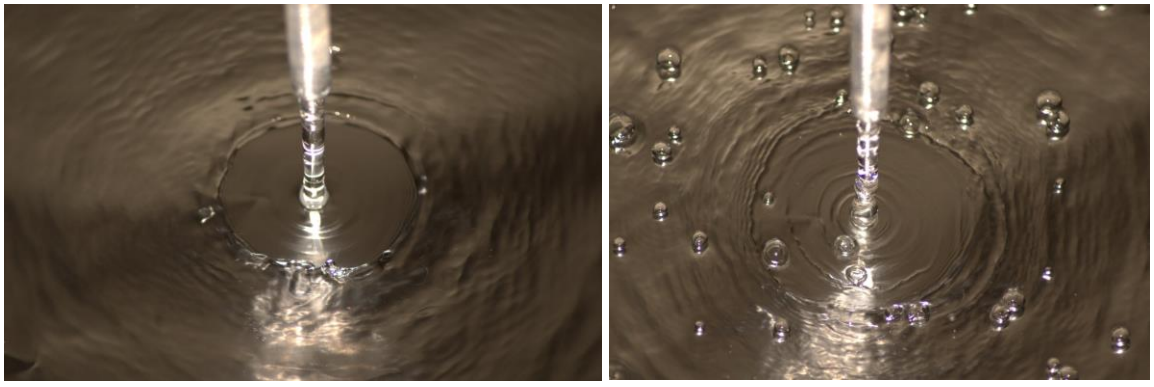

(a) β = 0 **(b) β = 0.2**

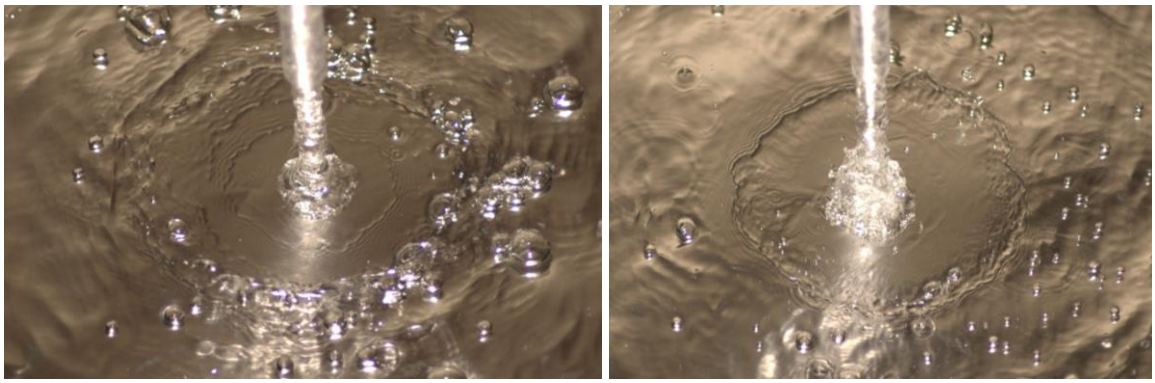

(c) β = 0.6 **(d) β = 0.9**

Figure 21: Nozzle discharge and hydraulic jump flow patterns for various β at Re_w = 4,329.

Comparing the results from the stagnation point pressure, Figure 20, and the dimensionless hydraulic jump diameter, Figure 19, it is clear that the diameter is a function of the pressure alone. The correlation of the normalized hydraulic jump diameter has the following form:

$$\frac{d_{hj}}{d} = 1.2P^*_{stag} \tag{3}$$

where $P^*_{stag}\left(=P_{stag,\beta}/P_{stag,\beta=0}\right)$ is the normalized stagnation pressure which is the ratio of two phase to single phase. The above correlation can be used for $1.0 \leq P^*_{stag} \leq 2.6$. The correlation of the dimensionless hydraulic jump diameter was compared with the experimental results, and matched with the experimental results within ±25%, as shown in Figure 22. This correlation shows that stagnation pressure governs the hydraulic jump of two-phase impinging jets.

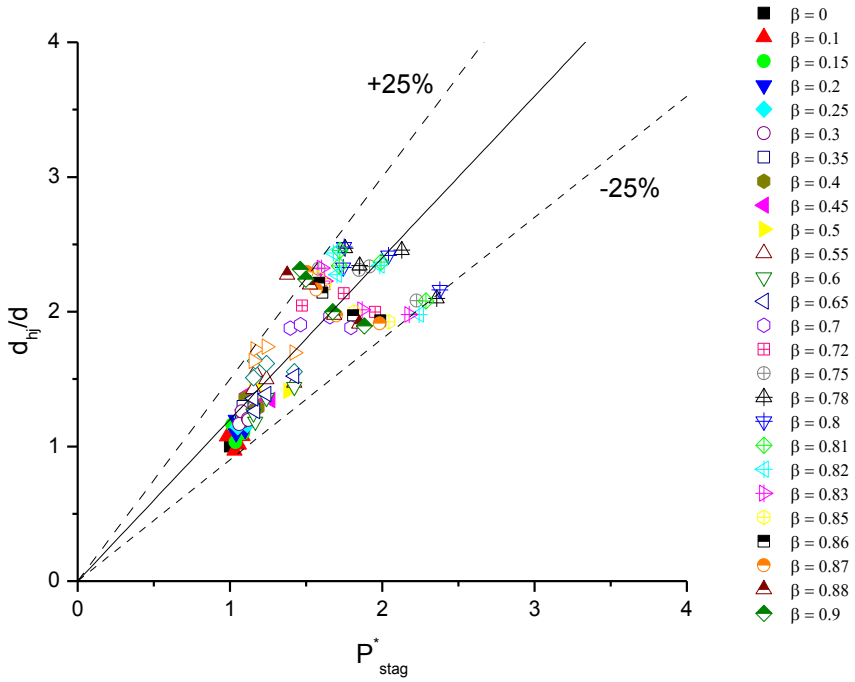

Figure 22: Correlation between dimensionless hydraulic jump diameter and pressure.

3.3 NUSSELT NUMBER AND PRESSURE

The variation of stagnation Nusselt number and normalized pressure with changing volumetric quality are shown in Figures 23 and 20 respectively. The results are similar to the dimensionless hydraulic jump and can be broken up into three regions; Region I is from β = 0 to β = 0.5, Region II is from β =0.5 to 0.8, Region III is from β = 0.8 to β = 0.9.

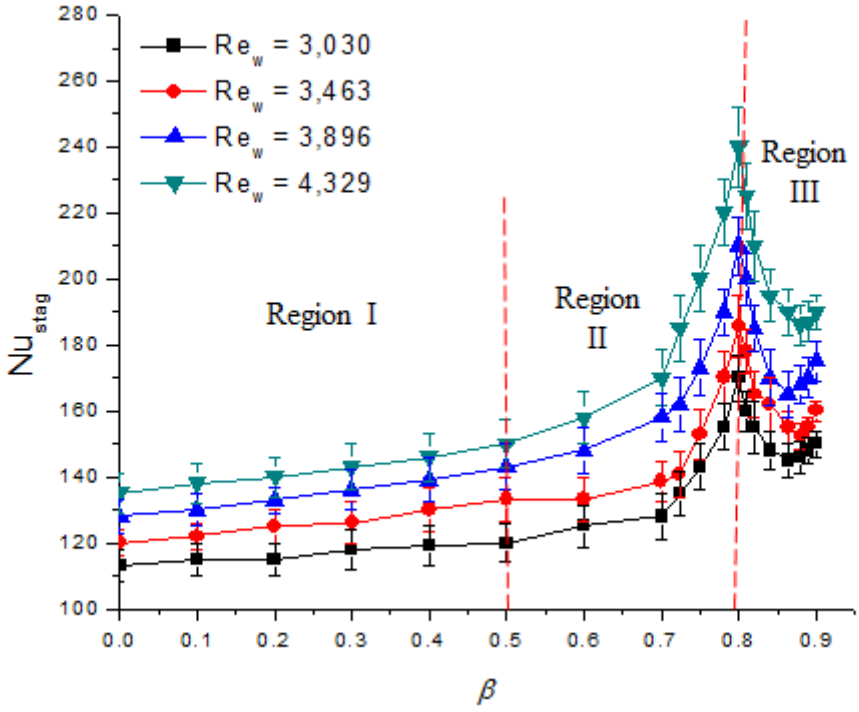

Figure 23: Stagnation Nusselt number as a function of the volumetric quality.

Region I in the stagnation Nusselt number and pressure show a linear increase as β increases towards Region II. This section of Nu_{stag} and P_{stag} has a gradual trend compared to the rest of the results from the experiment. Figure 23 shows the fluid flow patterns from pipe exit to impinged plate and Figure 26 shows the two-phase flow patterns inside of the nozzle. As shown in Figure 24 (a, b, c), the flow pattern at β = 0.1, 0.2 and 0.3 is bubbly flow. The fluid flow of the hydraulic jump and the free jet zone at this range, Figure 21 (b),

looks similar to a pure water impingement, Figure 21 (a). The stagnation zone can be easily compared between $\beta = 0$ and $\beta = 0.2$, which appears to be unaltered by the low β values.

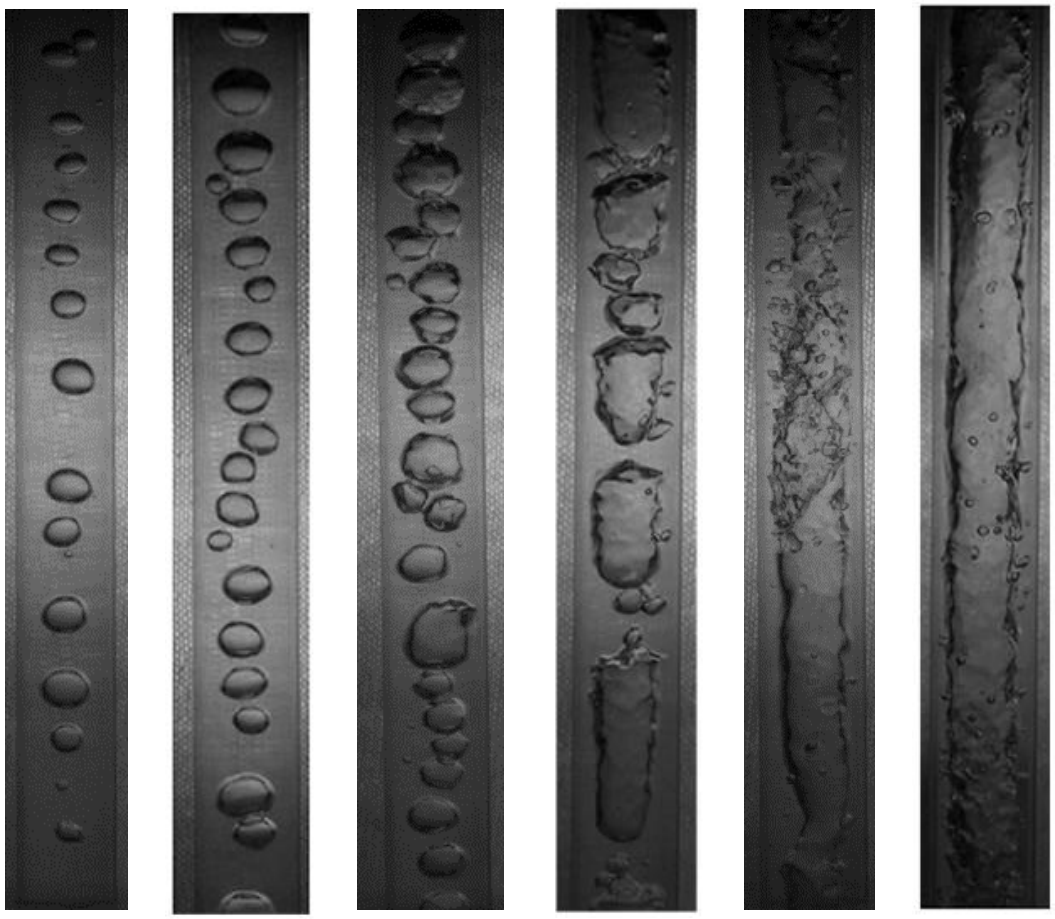

(a) $\beta = 0.1$ (b) $\beta = 0.2$ (c) $\beta = 0.3$ (d) $\beta = 0.6$ (e) $\beta = 0.8$ (f) $\beta = 0.9$

Figure 24: Flow patterns inside of the nozzle for various β at $Re_w = 4{,}329$.

In Region II, there was an exponential increase in the stagnation Nusselt number and pressure until they reach a β of around 0.75 to 0.81. At this point a peak was reached indicating that at a certain volumetric quality a maximum pressure and Nusselt number can be found. The Nusselt number increases by a factor of 1.7 at this range than that of the single phase value. There were also a greater number of visible slug bubbles which stay intact past the impingement zone and into the hydraulic jump as shown in Figure 21 (c)

and 24 (d). This figure shows an enlarged hydraulic jump diameter compared to both β = 0 and β = 0.2.

Region III appears after a volumetric quality of β = 0.8. A sharp decrease in both pressure and Nusselt number can be seen in this region. This can possibly be due to the water jet column distortion as it exits the nozzle with a smaller hydraulic jump size as shown in Figure 21 (d). This region had a larger fluctuating Nusselt number and pressure caused by water jet column distortion with high air velocity.

Comparing the results from the normalized stagnation pressure, Figure 20, and the stagnation Nusselt number, Figure 23, it is clear that the Nusselt number is a function of the normalized pressure alone. The correlation of the normalized Nusselt number has the following form:

$$\mathrm{Nu}^{*}_{stag} = 0.85 P^{*}_{stag} \tag{4}$$

where $\mathrm{Nu}^{*}_{\mathrm{stag}} \left(= \mathrm{Nu}_{\mathrm{stag},\,\beta} / \mathrm{Nu}_{\mathrm{stag},\,\beta=0}\right)$ and $P^{*}_{stag} \left(= P_{stag,\beta} / P_{stag,\beta=0}\right)$ are the normalized stagnation Nusselt number and pressure which is the ratio of two phase to single phase. The above correlation can be used for $1.0 \leq P^{*}_{stag} \leq 2.6$. The correlation of the normalized stagnation Nusselt number was compared with the experimental results, and matched with the experimental results within ±20%, as shown in Figure 25. This correlation shows that stagnation pressure governs the Nusselt number of two-phase impinging jets.

Figure 26 shows the lateral variation of Nusselt number and dimensionless hydraulic jump diameter at $\mathrm{Re_w}$ = 4,329, 3,896, 3,463 and 3,030. Nusselt number sharply decreases from stagnation point to hydraulic jump with high heat transfer rate. High heat transfer rate is obtained inside the hydraulic jump since there is a thin film with high flow velocity due to a dominant inertia force. At the outside of the hydraulic jump, Nusselt number

monotonically decreases since gravity is a dominant factor in this region. Maximum Nusselt number and hydraulic jump diameter are obtained at volumetric quality of 0.8.

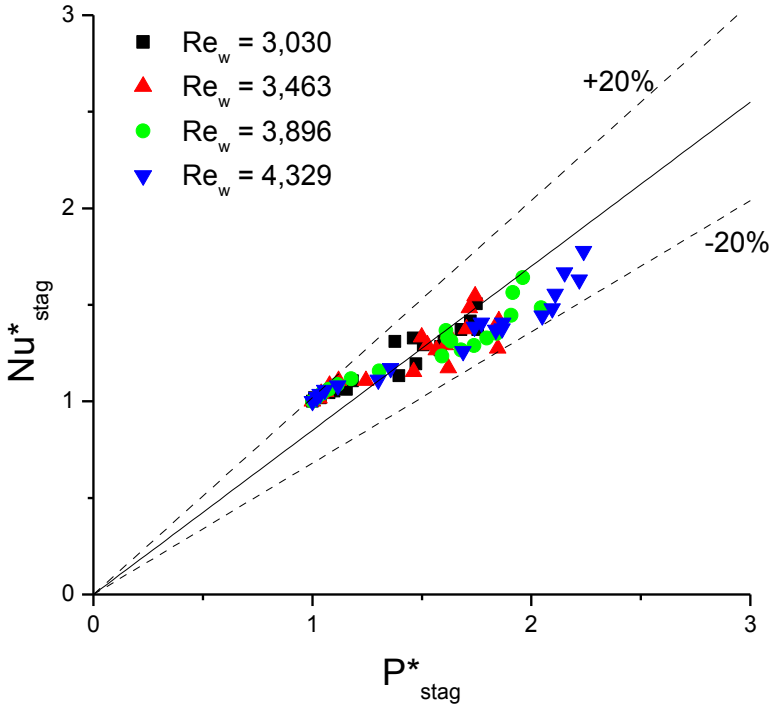

Figure 25: Correlation between the normalized stagnation Nusselt number and pressure.

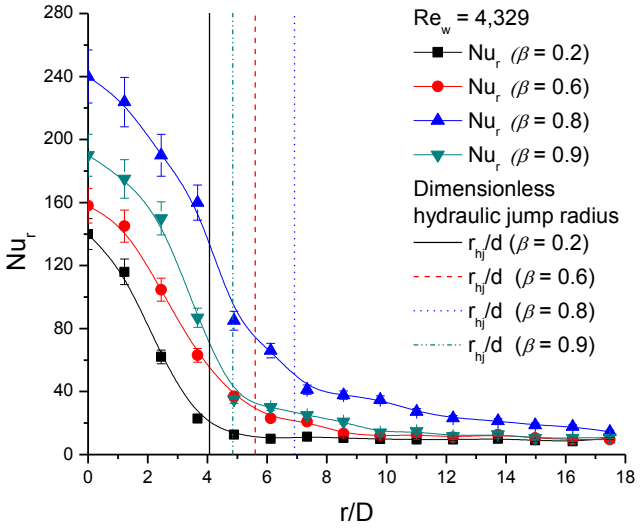

(a) Re_w = 4,329

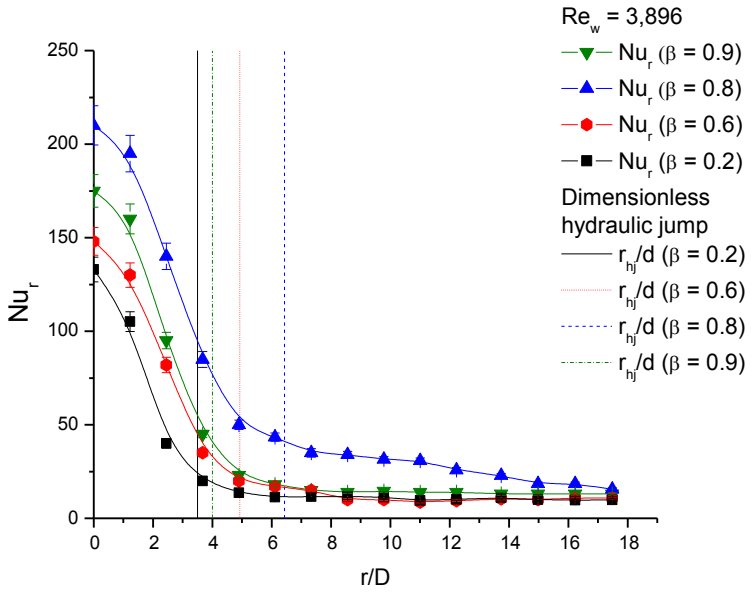

(b) Re_w = 3,896

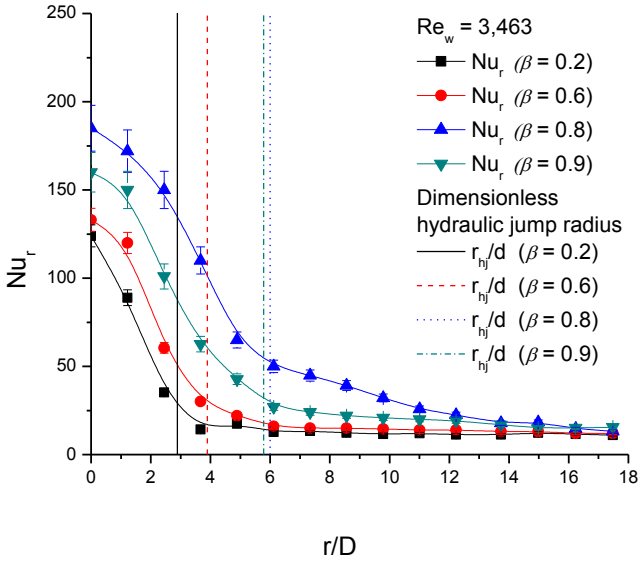

(c) Re_w = 3,463

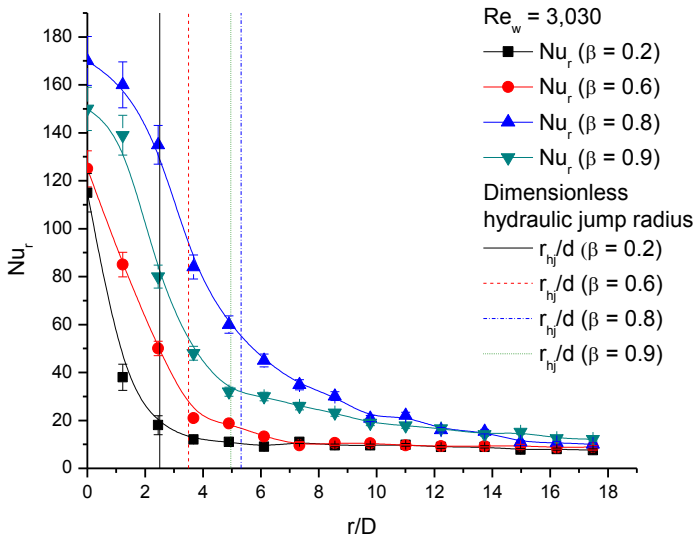

(d) $Re_w = 3{,}030$

Figure 26: Lateral variation of the local Nusselt number.

CHAPTER IV

CONCLUSION AND FUTURE WORK

A hydraulic jump is a phenomena which occurs when a supercritical flow slows and becomes a subcritical flow. Researchers have studied hydraulic jumps due to their super critical flow inside of the jump diameter, the high velocity in the region produces a large heat transfer rate. This phenomena occurs with impinging jet flow and can be influenced by the surface (i.e. roughness, attack angle, and shape) and the original flow velocity.

This research conducted extensive background review to gain a better understanding of the fluid flow and heat transfer characteristics of impinging jets and the hydraulic jump phenomena. It was found that impinging jets have a much higher heat transfer rate as compared to an ordinary channel flow. Free impinging jets were discussed along with confined and submerged impinging jets to compare their heat transfer and fluid flow characteristics. Impinging jets are used in a variety of applications, but this study focuses on the impinging jet as a means to cool a surface (i.e. electronics).

Other researchers studied that two phase flow can offer a higher rate of heat transfer than single phase flow. Even though there have been prior studies on two phase impinging jets, the effect of volumetric quality on the relationship of Nusselt number, hydraulic jump, and stagnation pressure for two-phase impinging jets have not been thoroughly studied (or understood). The objective of this study was to experimentally investigate the effect of volumetric quality of water on the hydraulic jump and heat transfer characteristics using impinging jets.

In this study, the heat transfer characteristics of air-assisted water jet impingement were experimentally investigated using water and air as the test fluid. The effects of volumetric quality ($\beta = 0 – 0.9$) on the Nusselt number and pressure were considered under fixed water-flow-rate condition. Four fixed flow rates were considered with Reynolds numbers of 3,030, 3,463, 3,896, and 4,329. A nozzle diameter of 5.86 mm was used to direct the impinging jet normal to the surface of the impinging surface at a height to diameter ratio of 1.

The results can be broken up into three regions; Region I is from $\beta = 0$ to $\beta = 0.5$, Region II is from $\beta = 0.5$ to 0.8, Region III is from $\beta = 0.8$ to $\beta = 0.9$. Region I, stagnation Nusselt number increased linearly as β was increased due to increase in number of bubbles. Region II, the stagnation Nusselt number increased exponentially as β increased, which is in slug flow region. This region also ends at the peak location for the stagnation Nusselt number. Region III starts at the peak location for the stagnation Nusselt number which then rapidly decreases until $\beta = 0.9$ is reached due to distortion of jet column.

In addition, it was found that the stagnation Nusselt number of two phase impinging jet is governed by the stagnation pressure and the lateral variation of Nusselt number is governed by hydraulic jump diameter. Based on the experimental results, a new correlation for the normalized Nusselt number of the impinging jet is developed as a function of the normalized stagnation pressure alone.

The findings from this study can be used for cooling applications such as electronics cooling to increase the overall heat transfer performance. Future study could investigate the impinging surface material characteristics for two phase impinging jet flow. The limitations in this study should also be addressed in future work. The limitations were caused by the test section (i.e.) Reynolds number range and heater temperature. A small

range of Reynolds numbers were studied due to the size of the impinging plate, increasing this range would result in a more complete understanding of the fluid flow and heat transfer characteristics. The heater temperature used was limited by the power supplied and by the risk of damaging the heater and impinging plate. If the heater temperature could be increased it would give more extreme temperature differences which could increase the accuracy of the results.

CHAPTER V

REFERENCES

Abdel-Fattah, A., M. Abd El-Baky, Numerical investigation of impinging two dimensional on an inclined flat plate, International Journal of Fluid Mechanics Research 35 (2009) 391-413.

Abdel-Fattah, A., Numerical and experimental study of turbulent impinging twin-jet flow, Experimental Thermal and Fluid Science 31 (2007) 1061-1072.

Akansu, Y.E., M. Sarioglu, K. Kuvvet, T. Yavuz, Flow field and heat transfer characteristics in an oblique slot jet impinging on a flat plate, Int. Communications in Heat Mass Transfer 35 (2008) 873-880.

Al-Hadhrami, L.M., S.M. Shaahid, Ali Mubarak, Heat transfer in a channel with inclined target surface cooled by single array of impinging jets, Proceedings of the ASME Turbo Expo, Montreal, Canada (2007) 35-42.

Al-Hadhrami, L.M., Study of heat transfer distribution in a channel with inclined target surface cooled by a single array of staggered impinging jets, Heat Transfer Engineering 31 (2010) 234-242.

Baonga, J.B., H. Louahlia-Gualous, M. Imbert, Experimental study of the hydrodynamic and heat transfer of free liquid jet impinging a flat circular heated disk, Appl. Therm. Eng. 26 (2006) 1125–1138.

Baydar, E., Y. Ozmen, An experimental investigation on flow structures of confined and unconfined impinging air jets, Heat Mass Transfer 42 (2006) 338-346.

Beitelmal, A.H., M.A. Saad, C.D. Patel, The effect of inclination on the heat transfer between a flat surface and an impinging two-dimensional air jet, International Journal of Heat and Fluid Flow 21 (2000) 156-163.

Bush, J.W.M., J.M. Aristoff, A.E. Hosoi, An Experimental investigation of the stability of the circular hydraulic jump, J. Fluid Mech. 558 (2006) 33-52.

Cengel, Yunus A., and Afshin J. Ghajar. Heat and Mass Transfer: Fundamental and Applications. New Delhi: McGraw Hill Education, 2011. Print.

Chang, C.T., G. Kojasoy, F. Landis, and S. Downing, Confined single- and multiple-jet impingement heat transfer—II. Turbulent two-phase flow, Int. J. Heat Mass Transfer 38 (1995) 843–851.

Chang, H. C., E.a. Demekhin, P.v. Takhistov, Circular Hydraulic Jumps Triggered by Boundary Layer Separation, Journal of Colloid and Interface Science 233.2 (2001): 329-338.

Chanson, H., Current knowledge in hydraulic jumps and related phenomena. A survey of experimental results, Eur. J. Mech. B/Fluids 28 (2009) 191–210.

Choo, K., Friedrich B. K., A.W. Glaspell, K. Schilling, "The Influence of Nozzle-to-plate Spacing on Heat Transfer and Fluid Flow of Submerged Jet Impingement," International Journal of Heat and Mass Transfer 97 (2016), 66 – 69.

Choo, K., S. J. Kim, Heat transfer and fluid flow characteristics of two-phase impinging jets, International Journal of Heat and Mass Transfer 53 (2010) 5692-5699.

Choo, K., S.J. Kim, Heat Transfer and Fluid Flow Characteristics of Nonboiling Two-Phase Flow in Microchannels, ASME Journal of Heat Transfer 133 (2011) 102901.

Choo, K., S.J. Kim, The influence of nozzle diameter on the circular hydraulic jump of liquid jet impingement, Experimental Thermal and Fluid Science 72 (2016) 12–17.

Craik, A., R. Latham, M. Fawkes, P. Gibbon, The circular hydraulic jump, J. Fluid Mech. 112 (1981) 347–362.

Friedrich, B. K., A. W. Glaspell, K. Choo, The Hydraulic Jump of Air-assistant Circular Impinging Jets, Experimental Thermal and Fluid Science, Under review.

Gardon, R., J.C. Akfirat, "Heat transfer characteristics of impinging two dimensional air jets," J. Heat Transfer, 88, pp. 101-108, (1966).

Gardon, R., J.C. Akfirat, "The role of turbulence in determining the heat transfer characteristics of impinging jets," Int. J. Heat Mass Transfer, 8, pp. 1261-1272, (1965).

Garimella, S., Air cooling technology for electronic equipment, CRC Press, 1996.

Godwin, R.P., The hydraulic jump ("shocks" and viscous flow in the kitchen sink), Am. J. Phys. 61 (9) (1993) 829–832.

Goldstein, R.J., M.E. Franchett, Heat transfer from a flat surface to an oblique im-pinging jet, ASME J. Heat Transfer 110 (1988) 84-90.

Hall, D.E., F.P. Incropera, R. Viskanta, Jet impingement boiling from a circular free surface jet during quenching; Part 2 – two-phase jet, ASME J. Heat Transfer 123 (2001) 911-917.

Incropera, Frank P., and David P. DeWitt, Fundamentals of Heat and Mass Transfer, New York: J. Wiley & Sons, 2002. Print.

Johnson, M., D. Maynes, J. Crockett, Experimental characterization of hydraulic jump caused by jet impingement on micro-patterned surfaces exhibiting ribs and cavities, Experimental Thermal and Fluid Science 58 (2014) 216-223

Kline, S.J., F.A. McClintock, Describing uncertainties in single sample experiments, Mech. Eng. 75 (1) (1953) 3–8.

Lee, D.H., S.J. Kim, Y. H. Kim, H. J. Park, "Heat transfer with fully developed slot jets impinging on confined concave and convex surfaces," Int. J. Heat and Fluid Flow, 88 pp. 218-223, (2015).

Lienhard, John H., (Mech Eng Mit) 2376 2001 Oct 19 12:23:28. C:textindia_2006jets.dvi (n.d.)

Liu, X., J.H. Lienhard, The hydraulic jump in circular jet impingement and in other thin liquid films, Exp. Fluids 15 (1993) 108–116.

Louahlia-Gualous, H., J.B. Baonga, Experimental study of unsteady local heat transfer for impinging miniature jet, Heat Transfer Eng. 29 (9) (2008) 782–792.

Lytle, D., B.W. Webb, Air jet impingement heat transfer at low nozzle-plate spacings, Int. J. Heat Mass Transfer 37 (1994) 1687-1697.

Martin, H., Heat and mass transfer between impinging gas jets and solid surface, Adv. Heat Transfer 13 (1977) 1-60.

Maynes, D., M. Johnson, B.W. Webb, Free-surface liquid jet impingement on rib patterned superhydrophobic surfaces, Physics of Fluids 23, 052104 (2011)

ME Case Studies, FM3 Hydraulic Jump through a Sluice Gate, N.p., 15 October 2011. Web. 07 Apr. 2016.

Mikielewicz, J., D. Mikielewicz, A simple dissipation model of circular hydraulic jump, Int. J. Heat Mass Transfer 52 (2009) 17–21.

Mubarak, Ali, S.M. Shaahid, Luai M. Al-Hadhrami, Impact of jet Reynolds number and feed channel geometry on heat transfer in a channel with inclined target surface cooled by single array of centered impinging jets with outflow in both directions, Proc. of International Conference of Mechanical Engineering, London, U.K, (2011) 6-8.

Obot, N.T., W.J.M. Douglas, A.S. Majumdar, Effect of semi confinement on impingement heat transfer, Procs. 7th Int. Heat Transfer Conf. 3 (1982) 395-400.

Pence, D.V., P.A. Boeschoten, J.A. Liburdy, Simulation of compressible micro-scale jet impingement heat transfer, ASME J. Heat Transfer 125 (2003) 447-453.

Polat, S., B. Huang, A.S. Majumdar, W.J.M. Douglas, Numerical flow and heat transfer under impinging jets: A Review, Ann. Rev. Num. Fluid Mech. Heat Transfer 2 (1989) 157-197.

Serizawa, A., O. Takahashi, Z. Kawara, T. Komeyama, I. Michiyoshi, Heat transfer augmentation by two-phase bubbly flow impinging jet with a confining wall, Proceedings of the 9th Int. Heat Transfer Conference, Jerusalem, 1990, pp. 93–98.

Stevens, J., B.W. Webb, Local heat transfer coefficients under an axisymmetric, single-phase liquid jet, ASME J. Heat Transfer 113 (1991) 71–78.

Trainer, D.G., J. Kim, S.J. Kim, Heat transfer and flow characteristics of air-assisted impinging water jets, International Journal of Heat and Mass Transfer 64 (2013) 501-513.

Viskanta, R., Heat transfer to impinging isothermal gas and flame jets, Exp. Therm. Fluid Sci. 6 (1) (1993) 111-134.

Watson, E.J., The radial spread of a liquid over horizontal plane, J. Fluid Mech. 20 (1964) 481–500.

Webb, B.W., C. F. Ma, Single-phase liquid jet impingement heat transfer, Adv. Heat Transfer 26 (1995) 105-217.

Yan, X., N. Saniei, Heat transfer from an oblique impinging air jet to a flat plate, Int. J. Heat and Fluid Flow 8 (6) (1997) 591-599.

Zhao, J., R.E. Khayat, Spread of a non-Newtonian liquid jet over a horizontal plate, J. Fluid Mech. 613 (2008) 411–443.

Zuckerman, N., and N. Lior. "Jet Impingement Heat Transfer: Physics, Correlations, and Numerical Modeling." Advances in Heat Transfer (2006): 565-631.

Zumbrunnen, D.A., M. Balasubramanian, Convective heat transfer enhancement due to gas injection into an impinging liquid jet, ASME J. Heat Transfer 117 (1995) 1011-1017.